Application of Additive Plasma Transferred Arc Surfacing for 3D Printing of Large-Scale Metal Products and Structures for Aerospace Applications (Review)

Volodymyr Korzhyk
China-Ukraine Institute of Welding, Guangdong Academy of Sciences
E.O. Paton Electric Welding Institute, National Academy of Sciences of Ukraine

Shiyi Gao*
China-Ukraine Institute of Welding, Guangdong Academy of Sciences

Vladyslav Khaskin
China-Ukraine Institute of Welding, Guangdong Academy of Sciences
E.O. Paton Electric Welding Institute, National Academy of Sciences of Ukraine

Oleksandr Bushma
E.O. Paton Electric Welding Institute, National Academy of Sciences of Ukraine

Andriy Alyoshin (junior)
E.O. Paton Electric Welding Institute, National Academy of Sciences of Ukraine

Xinxin Wang
China-Ukraine Institute of Welding, Guangdong Academy of Sciences

Oleksandr Bozhok
E.O. Paton Electric Welding Institute, National Academy of Sciences of Ukraine

Yanchao Hu
E.O. Paton Electric Welding Institute, National Academy of Sciences of Ukraine

Guirong
E.O. Paton Electric Welding Institute, National Academy of Sciences of Ukraine

The growing importance of 3D printing of finished metal products in recent years stems from its potential to reduce material costs in manufacturing and machining, facilitate changes in part size and product range, and enable the production of solid parts with complex internal geometries. Additive plasma transferred arc surfacing (APTAS) using wire and powder materials is a promising 3D printing process that combines the productivity of arc surfacing processes with the forming accuracy approaching that of beam-based processes. Therefore, this work analyzes the current state of scientific research on the additive manufacturing of metal parts from steels and alloys, including the fabrication of aerospace structures. It also identifies promising directions for the further development of this manufacturing approach and explores the design of innovative plasma and microplasma equipment for the technological implementation of these identified prospects.

INTRODUCTION, AIM, AND OBJECTIVES OF THE ARTICLE

In recent years, a qualitative leap has occurred in the application of 3D printing processes, transitioning from the creation of prototype models for metal product manufacturing to the direct printing of such products using various metals and alloys [1-3]. Modern additive manufacturing (AM) is an innovative manufacturing process that enables the production of complex, near-net-shape 3D parts of the required size directly from CAD models, eliminating the need for dies or complex machining. This results in reduced manufacturing time, waste, and final cost. For example, the cost of additively manufacturing certain titanium aerospace components is half the cost of manufacturing them from forged stock [4]. Another significant application of additive manufacturing lies in the military domain. This type of manufacturing enables the rapid and uncontrolled replication of highly complex instruments of warfare, necessitating novel strategies from military organizations and governments [5]. Consequently, owing to its exceptional flexibility and adaptability in addressing a broad spectrum of industrial challenges, additive manufacturing is gaining increasing prominence in the contemporary world [6-8].

In contemporary additive manufacturing, the following processes are predominantly employed to fabricate finished metal components, arranged in ascending order of productivity and weld pool dimensions [1, 4]: selective laser melting (SLM), electron beam selective melting (EBSM), and wire arc additive manufacturing (WAAM). Plasma arc welding (PAW), which can utilize either filler wires or powders [9, 10], exhibits comparable productivity and weld pool characteristics to the WAAM process. A significant gap exists between SLM and WAAM processes regarding productivity, forming accuracy, and the surface roughness of finished products. EBSM and PAW processes can occupy an intermediate position; however, EBSM implementation necessitates complex and costly vacuum chambers, which limit the finished product's size. Traditional PAW processes, in terms of the specified parameters, are comparable to WAAM processes. Ideally, manufacturers would have an additive manufacturing process that combines forming accuracy and surface roughness comparable to SLM, while maintaining productivity close to WAAM. Additive plasma transferred arc surfacing (APTAS) – additive plasma or microplasma surfacing by direct arc – could be such a process. In this process, powder or wire materials can be used for 3D printing of aerospace equipment parts [11, 12]. Specifically, heat-resistant nickel alloys and titanium-based alloys are used in the manufacture of aircraft engine components [13].

This study aims to analyze the current state of scientific research on the additive manufacturing of metal parts using steels and alloys. It identifies promising directions for the future development of such manufacturing, particularly the additive plasma transferred arc surfacing (APTAS) process. Additionally, it encompasses the design of innovative plasma and microplasma equipment for the technological realization of the identified prospects.

To achieve this goal, the study addressed the following tasks:

1. Analysis of the key features and effectiveness of additive plasma transferred arc surfacing (APTAS) for 3D printing applications.
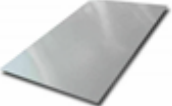
2. Review of current research on APTAS for large-scale product manufacturing using steels and iron- and nickel-based alloys.
3. Review of current research on APTAS for large-scale product manufacturing using aluminum alloys.
4. Review of current research on APTAS for large-scale product manufacturing using titanium alloys.
5. Review of current research on hybrid and combined 3D printing methods incorporating APTAS technologies.
6. Identifying new opportunities for applying APTAS to the additive manufacturing of aerospace structures.

MAIN FEATURES OF ARC ADDITIVE CLADDING TECHNOLOGIES AND THE EFFICIENCY OF APPLYING APTAS TECHNOLOGIES TO 3D PRINTING

Microplasma and plasma arc surfacing processes, utilizing both powder and wire filler materials, can be implemented for plasma arc technologies [14, 15]. A microplasma process typically utilizes a compressed, low-current (up to 50-80 A) arc that burns within a laminar flow of inert gas. APTAS, conversely, employs a current in the range of 50-150 A. In both instances, the compressed arc current can be either constant or modulated, with reverse polarity being a specific example. This reverse polarity modulation is particularly applicable in the welding and surfacing of aluminum alloys.

As demonstrated by the comparison presented in study [16] (Table 1), SLM technology is advisable when seeking to achieve the highest accuracy in three-dimensional product shape and minimize surface roughness. When maximum productivity is paramount, WAAM (Wire + Arc Additive Manufacturing) technology is suitable. Plasma powder additive surfacing (3DPDM or APTAS with powders) offers a compromise between quality and productivity. However, when using conventional arc plasma, the quality may be even lower than when using WAAM with a consumable electrode arc [17, 18]. Therefore, improving the manufacturing quality of three-dimensional products is crucial, and the application of microplasma offers a potential solution.

TABLE 1
COMPARISON OF THE BASIC CHARACTERISTICS OF THE MAIN ADDITIVE MANUFACTURING PROCESSES [16]

Production Process	SLM	WAAM	3DPDM (APTAS)	Sheet Metal
Material	316L (1.4403)			
Initial State	Powder (30-63 μm)	Wire (1.2 mm diameter)	Powder (50-125 μm)	Cold-Rolled Sheet
Surfacing Source	Laser	Electric Arc	Electric Arc	-
Layer Height/Sheet Thickness	0.06 mm	1.7 mm	0.97 mm	6 mm
Process Time	231.3 min	13.5 min	25.5 min	-
Reference component				

Additive manufacturing processes utilizing plasma arc technologies (Plasma Transferred Arc Welding - PTA) offer several advantages over competing technologies. These advantages include high-quality deposited layers, high speed and, consequently, high productivity, and the ability to regulate the width of the growing layer [19]. The primary competitors of the PTA process are the Wire Arc Additive Manufacturing (WAAM) processes and Cold Metal Transfer (CMT). In terms of heat input into the growing product, PTA occupies an intermediate position between WAAM, which has significant heat input, and CMT, which has the least. However, compared to cold metal transfer (CMT), which exclusively utilizes wire, plasma arc processes accommodate both wire and powder additives, thereby significantly expanding their technological capabilities.

The wire arc additive manufacturing (WAAM) process can be implemented not only using a consumable electrode arc, but also through gas tungsten arc welding (GTAW) or plasma arc welding (PAW) processes, where the wire serves as filler material. Additive cladding with wire introduces the risk of generating specific defects (Fig. 1) [20]. To address these issues, mode selection, supplementary technological techniques such as hybrid 3D printing, and heat source modification are employed.

FIGURE 1
CORRELATION BETWEEN MATERIALS AND DEFECTS IN WAAM PROCESSES [8]
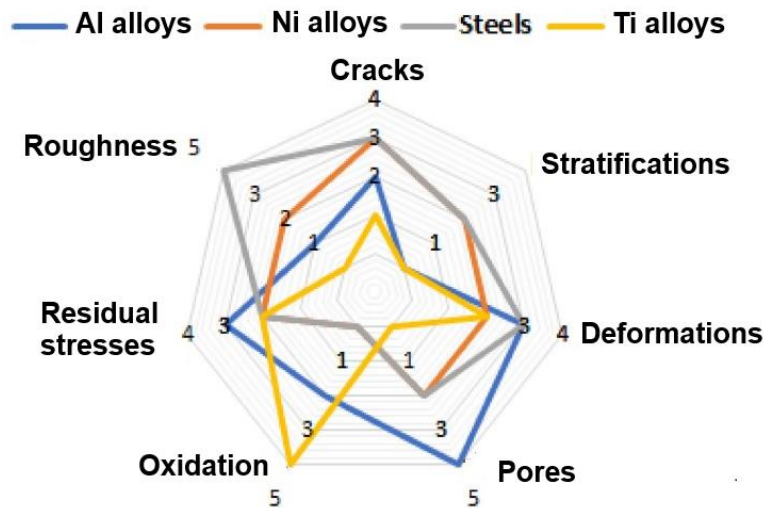
APPLICATION OF APTAS TECHNOLOGIES (3D PRINTING) FOR LARGE-SCALE METAL PRODUCT FABRICATION

APTAS of Large-Scale Products Using Steels and Iron- and Nickel-Based Alloys

Additive manufacturing of 3D objects from iron- and nickel-based steels and alloys presents several challenges related to overheating during the surfacing process [21, 22]. For instance, CMT printing of 2Cr13 steel walls resulted in a small number of pores and no cracks across different layers, indicating a high degree of densification [23]. The deposited microstructure comprised martensite and ferrite, along with the $(Fe,Cr)_{23}C_6$ phase, which precipitates at the α-Fe grain boundaries. However, the martensite content gradually increased from the 5th to the 25th layer due to overheating, despite the partial decomposition of metastable martensite into stable ferrite via carbon atom diffusion. Hardness changed slightly from the 5th to the 15th layer and then increased rapidly from the 20th to the 25th layer. The fracture process transitioned from ductile (1st-10th layers) to mixed (15th-20th layers), ultimately resulting in brittle fracture (25th layer). Therefore, to establish a 3D printing process that consistently produces stable product structures, a modified technological approach is required. APTAS represents a promising option for achieving this.

Indeed, the APTAS process has been proposed for fabricating parts with enhanced wear resistance from intermetallic alloys, such as iron aluminide. Study [24] demonstrated the feasibility of manufacturing parts from an iron-nickel-aluminum intermetallic compound using this method. Study [25] proposes the use of 3DPMD (APTAS) plasma-arc technology for the additive manufacturing of wear-resistant functional layers on wear surfaces and tool bodies. These layers would be composed of nickel-based alloy Ni 625 and iron-based alloy PS Fe-hard D. Studies [26-28] propose plasma arc surfacing with wires (up to 120 A) and microplasma surfacing with powder materials (at a current of up to 50 A) for manufacturing products from carbon and stainless steels. Research on the fabrication of steel spatial primitives, including walls, cups, cones, and hemispheres, revealed that dimensional deviations remained within ±0.5 mm. Porosity ranged from 1% to 2%, while mechanical strength reached approximately 90% to 95% of cast metal. The deposited material exhibited a fine-grained, uniform structure with minimal interlayer mixing.

Utilizing pulsed-current plasma arc welding (PAW) for additive plasma transferred arc surfacing (APTAS) facilitates the printing of steel components with intricate geometries [29]. The grain structure of the deposited layers exhibits a transition from a relatively fine grain size near the substrate to a coarser structure with larger grains near the top of the additively clad sample. The sample's microstructure (Fig. 2) near the substrate comprised pearlite colonies (dark) and ferrite grains (light). The ferrite and pearlite grains were nearly equiaxed, ranging from 12 to 19 μm in size. In the sample's microstructure near the surface (Fig. 2), the light areas represent ferrite with distinct boundaries, while the dark areas represent pearlite, composed of a fine mixture of ferrite and iron carbide. The ferrite and pearlite grains exhibit a columnar morphology, with sizes ranging from 250 to 350 μm.

FIGURE 2
CROSS-SECTION OF A WALL FABRICATED VIA ADDITIVE SURFACING OF CARBON STEEL, SHOWCASING MICROSTRUCTURES WITH INCREASING GRAIN SIZE ALONG THE BUILD HEIGHT [29]
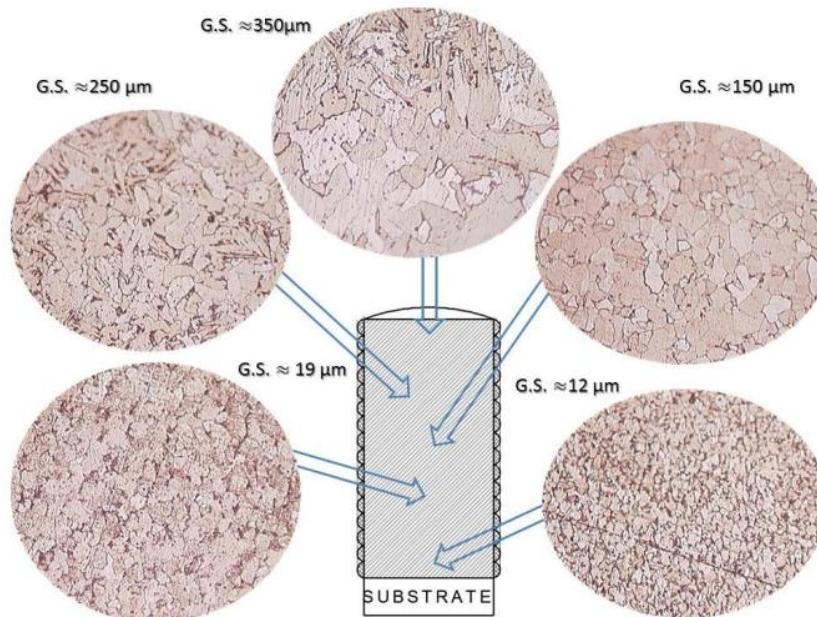
Printing precise products using the PAW method with steel shot exhibits relatively low productivity (approximately 50 g/h) when controlling product temperature and implementing cooling periods after each layer deposition. This approach enables control over grain size and hardness within the printed walls. Indeed, reducing the waiting time promotes larger grain size and decreased metal hardness as wall height

increases. Increasing the dwell time between deposited layers reduces the average grain size, while hardness increases [30].

Additive manufacturing of geometrically complex components from carbon and alloy steels utilizes three-dimensional plasma transferred arc surfacing (3DPMD or APTAS) with wire and powder feedstock. Specifically, 3DPMD (APTAS) multilayer surfacing of steels was employed to manufacture complex-shaped surfaces for a cross-rolling tool [31].

The APTAS method has been proposed for printing aircraft components using wires [32, 33] and powders [34-36] composed of heat-resistant, nickel-based alloys. Study [32] found that when 3D printing a ring-shaped aviation component using a filler wire composed of Cr25Ni60W14Ti alloy (EI868), the resulting microstructure corresponds to the normal state of the EI868 alloy. The fusion lines are not visible, and the structure is uniform with mutual intergrowth of grains between layers (Figure 3). The mechanical properties of the additively grown component are comparable to those of cast billets and forgings. At a temperature of 900°C, the properties are: $s_{0.2} = 35 \pm 5$ kgf/mm^2, $s_{B} = 49 \pm 5$ kgf/mm^2, and elongation (y) = $62 \pm 5\%$. No cracks or other critical metallurgical defects were found after machining the printed workpiece. Using APTAS for 3D printing an aircraft part blank resulted in an economic benefit of approximately \$3,800–\$4,000. Study [36] developed a microplasma APTAS method for repairing a D-18T aircraft engine using Cr35Ni55W5Mo3TiAlNb (EI648) alloy powder. This method achieved an economic benefit of approximately \$2,500, representing 23% of the cost of a new part.

FIGURE 3
(A) APTAS ADDITIVE SURFACING COMPLEX WITH A GROWN PART, (B) FINISHED PART AFTER MACHINING, (C) MICROSTRUCTURE OF THE DEPOSITED HEAT-RESISTANT ALLOY CR25NI60W14TI (EI868) [32]
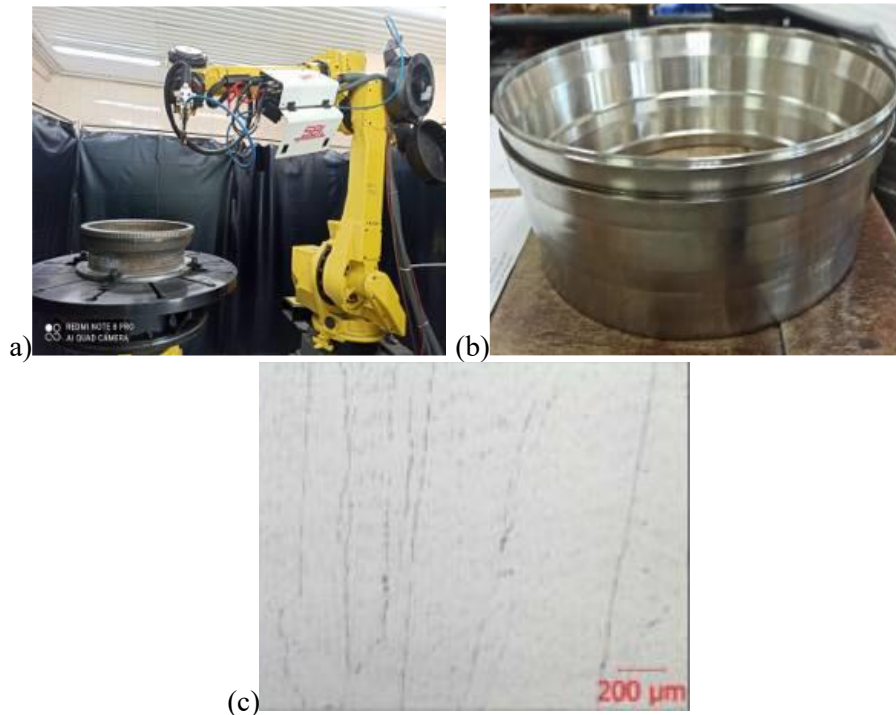
The study [37] proposed a microplasma APTAS technology using Cr35Ni55W5Mo3TiAlNb (EI648) alloy powder to eliminate casting defects, demonstrating a 3D printing application. The developed technology enabled the fabrication of a nickel alloy product exhibiting specific metallurgical phases and structures comparable to those found in cast shaped castings. These phases, including gamma solid solution, metastable carbides, and nitrides, significantly enhance the material's mechanical properties. Gamma solid

solution, renowned for its high resistance to deformation and restorative capacity, proves ideal for applications demanding high strength. Metastable carbides and nitrides enhance the alloy structure, providing additional wear resistance and resilience against external factors. This technology expands the possibilities for repairing and eliminating defects in large-scale cast components, including those made from nickel alloys.

APTAS of Large-Scale Products Made From Aluminum Alloys

A simpler approach to 3D printing aluminum products is using the WAAM process. One example is the printing of samples from the 5A06 alloy, as described in [38]. Mechanical studies of the printed products revealed anisotropic tensile properties in directions parallel and perpendicular to the texture orientation. The average ultimate tensile strength and yield strength in the direction perpendicular to the texture orientation are 251 MPa and 101 MPa, respectively. In the direction parallel to the texture orientation, these values are 239 MPa and 90 MPa, respectively. The average relative elongation values in directions parallel and perpendicular to the texture orientation are 37% and 34%, respectively. One approach to mitigating this anisotropy is employing an alternative 3D printing process.

Utilizing the TIG process for 3D printing aluminum products, such as those composed of the 2219-Al alloy, enables the achievement of isotropic mechanical properties [39]. However, the average tensile strength is only 237 MPa, representing just 57% of the alloy's potential. Analysis indicates that the insufficient tensile strength can be attributed to the absence of a strengthening effect during the printing process. Fracture observation reveals that the θ phase initiates crack formation. The study [40] demonstrates that 3D printing of aluminum products using the GTAW process encounters surfacing accuracy issues when employing lateral wire feeding. Additionally, when surfacing aluminum alloys using a non-consumable electrode process, filler wire alloying elements (primarily Mg) can burn out, reducing the finished product's mechanical properties. To enhance these properties when surfacing the Al-6.3Cu alloy, a production system employing a double wire and a non-consumable electrode arc was proposed in [41]. This system adds magnesium to the Al-Cu alloy, thereby improving its mechanical properties.

Figure 4 illustrates typical microstructures of additively clad layers for Al-Cu-Mg alloys with varying compositions. Each deposited layer is divided into an inner layer region and an interlayer region (Figures 4a, 4d, and 4g). The microstructure exhibits distinct morphological characteristics in these different regions. Within the inner layer, the microstructure primarily comprises coarse columnar grains and fine equiaxed grains, exhibiting a heterogeneous distribution of characteristics. As shown in Figures 4b and 4e, most grains are non-dendritic, with only a small number of dendritic grains present in the inner layer of the Al-3.6Cu-2.2Mg and Al-4Cu-1.8Mg alloys. In contrast, equilibrium and columnar dendritic grains become dominant in the inner layer region of the Al-4.4Cu-1.5Mg alloy (Figure 4h). The microstructure in the interlayer region is equilibrium non-dendritic in the Al-3.6Cu-2.2Mg (Figure 4c) and Al-4Cu-1.8Mg (Figure 4f) alloys, and equilibrium dendritic in the Al-4.4Cu-1.5Mg alloy (Figure 4i).

Various compositions of Al-Cu-Mg alloys were created by adjusting the feed rate of two binary wires: aluminum-copper ER2319 and aluminum-magnesium ER5087. This process yielded strengthening phases of $Al_2Cu + Al_2CuMg$ and Al_2CuMg with increased microhardness. This resulted in isotropic characteristics for ultimate tensile strength (UTS), yield strength (YS), and elongation. The UTS was approximately 280±5 MPa in both the horizontal and vertical directions for all specimens. The YS showed an increasing trend from 156 MPa to 187 MPa, while elongation decreased from 8.2% to 6%.

Applying the PAW process or its analogs for APTAS yields a result similar to that obtained with TIG or GTAW. One positive difference is that the PAW process allows for the use of both wire and powder materials. Simultaneously, the introduction of various filler materials facilitates in-situ alloying, occurring directly within the weld pool [42]. This approach utilizes variable wire feeding to additively manufacture structures possessing a graded chemical composition. The objective is to fabricate components with locally tailored mechanical and technological properties, effectively mitigating adverse side effects such as abrupt phase transformations and localized variations in thermal expansion coefficients.

FIGURE 4
MICROSTRUCTURES OF ADDITIVE CLADDING LAYERS OF AL-CU-MG SYSTEM ALLOYS [41]: (A) AL-3.6CU-2.2MG, (B) INTERNAL LAYER OF AL-3.6CU-2.2MG, (C) INTERMEDIATE LAYER OF AL-3.6CU-2.2MG, (D) AL-4CU-1.8MG, (E) INTERNAL LAYER OF AL-4CU-1.8MG, (F) INTERMEDIATE LAYER OF AL-4CU-1.8MG, (G) AL-4.4CU-1.5MG, (H) INTERNAL LAYER OF AL-4.4CU-1.5MG, (I) INTERMEDIATE LAYER OF AL-4.4CU-1.5MG
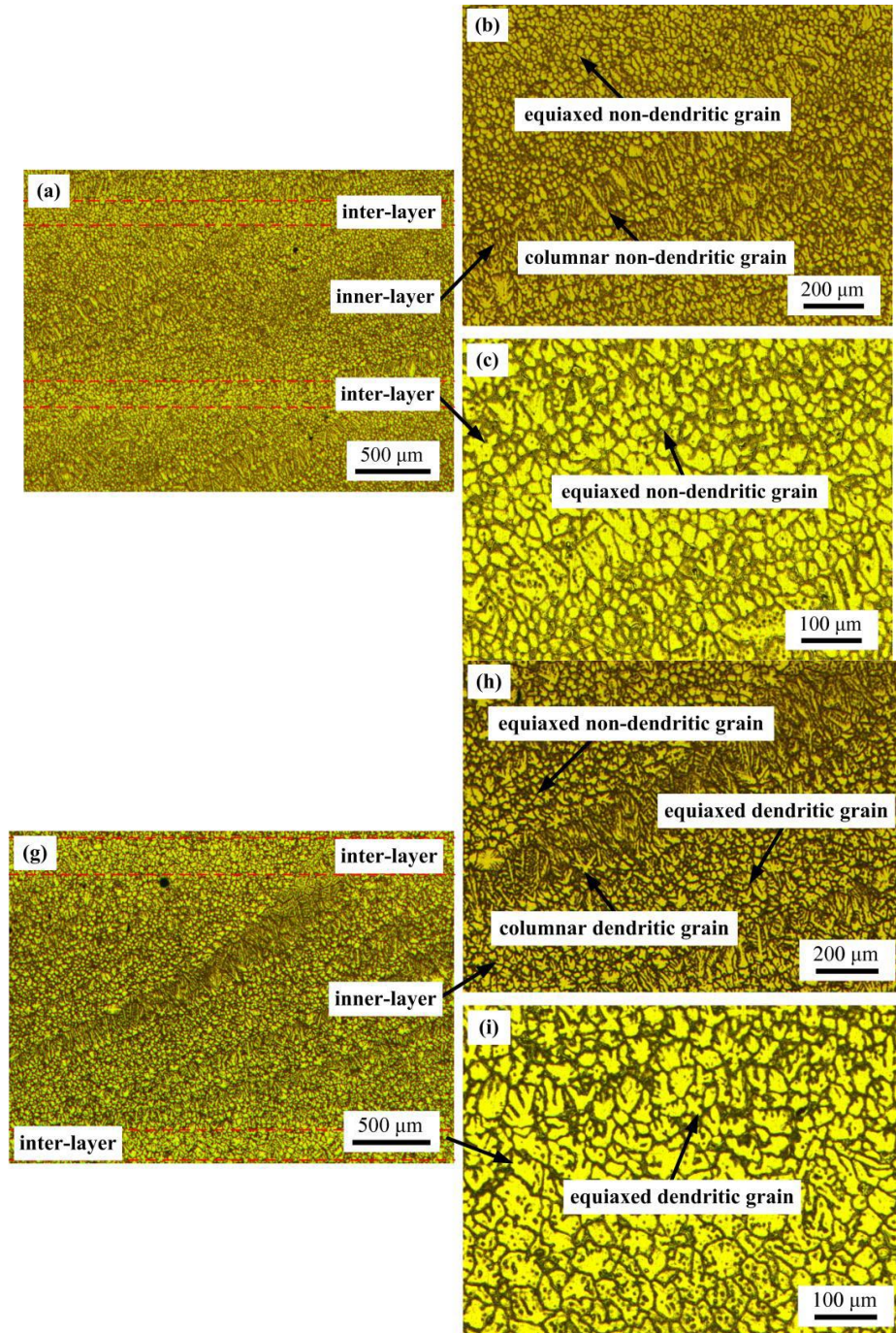
APTAS of Large-Scale Products Made From Titanium Alloys

Plasma transferred arc surfacing is an innovative additive manufacturing technique that combines plasma welding with wire feeding. In a study [43], a process utilizing Ti-6Al-4V alloy wires was developed. The plasma process enabled the fabrication of straight walls up to 17.4 mm thick. This resulted in a maximum effective wall width of 15.9 mm after machining, surpassing the performance of competing processes. The efficiency of Ti-6Al-4V surfacing averaged 93%, with a maximum deposition rate of 1.8 kg/h. During surfacing, coarse columnar grains grew from the substrate, transforming into a Widmanstätten lamellar structure upon cooling. Bands exhibiting a repeating basketweave microstructure of varying sizes were observed in the deposited layers (Fig. 5). The average microhardness was 387 HV, 12% higher than that of the substrate. This wire arc plasma surfacing process is intended for the additive manufacturing of large aerospace components.

FIGURE 5
FINE LAMELLAR STRUCTURE CHARACTERISTIC OF THE TOP PORTION OF ADDITIVELY SURFACED TI-6AL-4V ALLOY (ACICULAR LAMELLAE INDICATE THE PRESENCE OF MARTENSITE) [43]
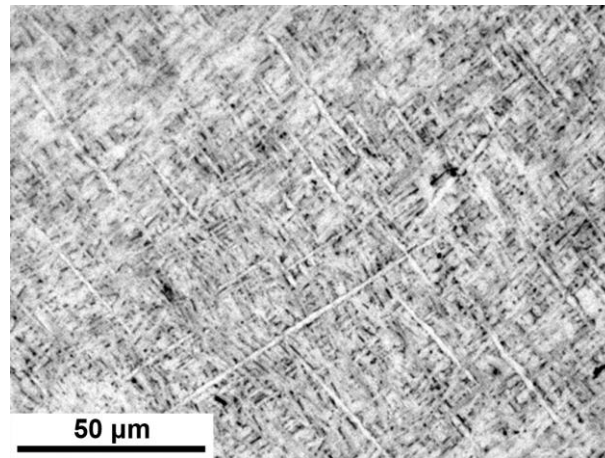
In the case of 3D printing with titanium alloys using WAAM processes, TIG or PAW processes are used as energy sources, unlike with steels and aluminum alloys [44]. Significant residual stresses can occur within each deposited layer, manifesting as distortion in the printed walls [45]. To mitigate these stresses, rolling each layer of the additively manufactured wall has been proposed. Neutronographic and contour measurements demonstrate that this approach reduces residual stresses, particularly at the substrate interface. Simultaneously, the microstructure was refined and improved. A similar approach to mitigating residual stresses was employed in [46]. Residual stress measurements indicated that, while the samples still exhibited tensile stresses (up to 500 MPa), their magnitude was reduced by 60%, particularly at the interface between the deposited layers and the substrate.

The APTAS process, utilizing Ti-6Al-4V titanium wires (PTA), is typically conducted on a substrate of the same material. The PTA wire feeding device is integrated with a 3-axis CNC machine for part fabrication. Controlling the evolution of residual stress within printed walls necessitates a combination of process parameter adjustments. In a study conducted by researchers at the Institut Laue-Langevin (ILL) in Grenoble, France [47], residual strains were measured using neutron diffraction (ND) on the SALSA instrument. Longitudinal stresses were determined using a coordinate measuring machine (CMM) in conjunction with the Euler-Bernoulli beam theory. Furthermore, optical microscopy (OM) analysis of part cross-sections was employed to investigate microstructure evolution. Results demonstrated the impact of varying interlayer holding times on residual stress evolution.

Study [48] revealed that minimizing deformation during each layer deposition is crucial for significant β-grain size reduction. Analysis of EBSD strain distribution in each layer and reconstruction of the prior β-grain structure demonstrated that the coarse, centimeter-scale, columnar β-grain structure can be refined to 100 μm. The deformation stage induces the development of new β-orientations through local inhomogeneities in the deformation texture. These inhomogeneities act as nuclei during the α→β transformation that occurs as each layer is reheated during the subsequent deposition pass.

To control the influence of heat accumulation on filler metal transfer, wall formation, and arc stability during wire and tungsten electrode arc additive manufacturing (GT-WAAM) of Ti6Al4V under localized gas shielding, an infrared pyrometer was used to measure interpass temperature [49]. This factor is key to determining heat accumulation. Arc stability and metal transfer were monitored using a high-speed camera. This approach enabled optimization and control of the additive printing process.

An innovative wire-based additive cladding process with forced inter-pass cooling using compressed CO_2 [50] has been proposed for fabricating thin-walled Ti6Al4V structures. Forced interpass cooling has been determined to not only improve surfacing properties but also contribute to geometric repeatability and enhanced production efficiency by reducing interlayer application time.

Additive plasma powder deposition (3DPMD or APTAS) is one of the most promising processes for manufacturing large-scale titanium components. The primary advantage, besides the capability to fabricate large-scale structures with lower material costs and investments compared to laser and electron beam processes, is the ability to manufacture parts from a wide range of materials [51]. Homogeneous titanium structures can be created without internal defects and with an acceptable surface finish. Even without optimizing for maximum productivity, a deposition rate of 170 cm³/h was achieved. This surpasses the capabilities of most beam methods. Furthermore, the stability of additive plasma transferred arc wire surfacing is critically dependent on the wire feeding mode into the weld pool [52].

Therefore, plasma arc surfacing presents itself as a highly promising approach for addressing the challenges of fabricating titanium alloy components in industries such as aerospace, automotive, and marine [53].

Hybrid and Combined 3D Printing Methods Utilizing APTAS Technologies

Utilizing commercially available welding wires does not always yield the desired deposited metal composition, particularly when creating a gradient functional structure. For instance, fabricating an integral working wheel for an aircraft engine, featuring a double helix composed of superalloy, necessitates a combined approach of plasma surfacing and mechanical milling [54]. Using powder results in a significant percentage of loss and makes it difficult to obtain a mechanically homogeneous mixture of powders with significantly different densities [55]. Hybrid utilization, combining the advantages of wire-based additive manufacturing with those of powder-based methods, presents a promising approach [56].

Indeed, if increasing the volume of deposited metal while maintaining a constant deposition rate through filler wire addition is technically unfeasible, productivity can be enhanced by supplementing with powder [20]. In this case, material utilization will be higher than when using only powder, and using wire will be more economically feasible than using powder of the same chemical composition. With hybrid APTAS using both wire and powder, the powder can be used as a reinforcing additive to increase the strength, hardness, and wear resistance of the part wall (Fig. 6) [57]. Hybrid plasma deposition with wire and powder enables the fabrication of gradient layers on titanium alloy components. Indeed, utilizing a TC4 (Ti-6Al-4V) filler wire with supplementary WC powder feeding facilitates hardness variation within the deposited layers, ranging from 32 HRC to 56 HRC.

FIGURE 6
MACROSTRUCTURES AND MICROSTRUCTURES OF THE WALL FABRICATED VIA PAW-WAAM IN ALL DIRECTIONS [57]: (A) OVERALL VIEW OF THE AIRCRAFT COMPONENT FRAGMENT. (B) MACROSTRUCTURE IN THE XY DIRECTION; (C) MACROSTRUCTURE IN THE XZ DIRECTION; (D) MACROSTRUCTURE IN THE YZ DIRECTION; (E) MICROSTRUCTURE IN THE XY DIRECTION; (F) MICROSTRUCTURE IN THE XZ DIRECTION; (G) MICROSTRUCTURE IN THE ZY DIRECTION
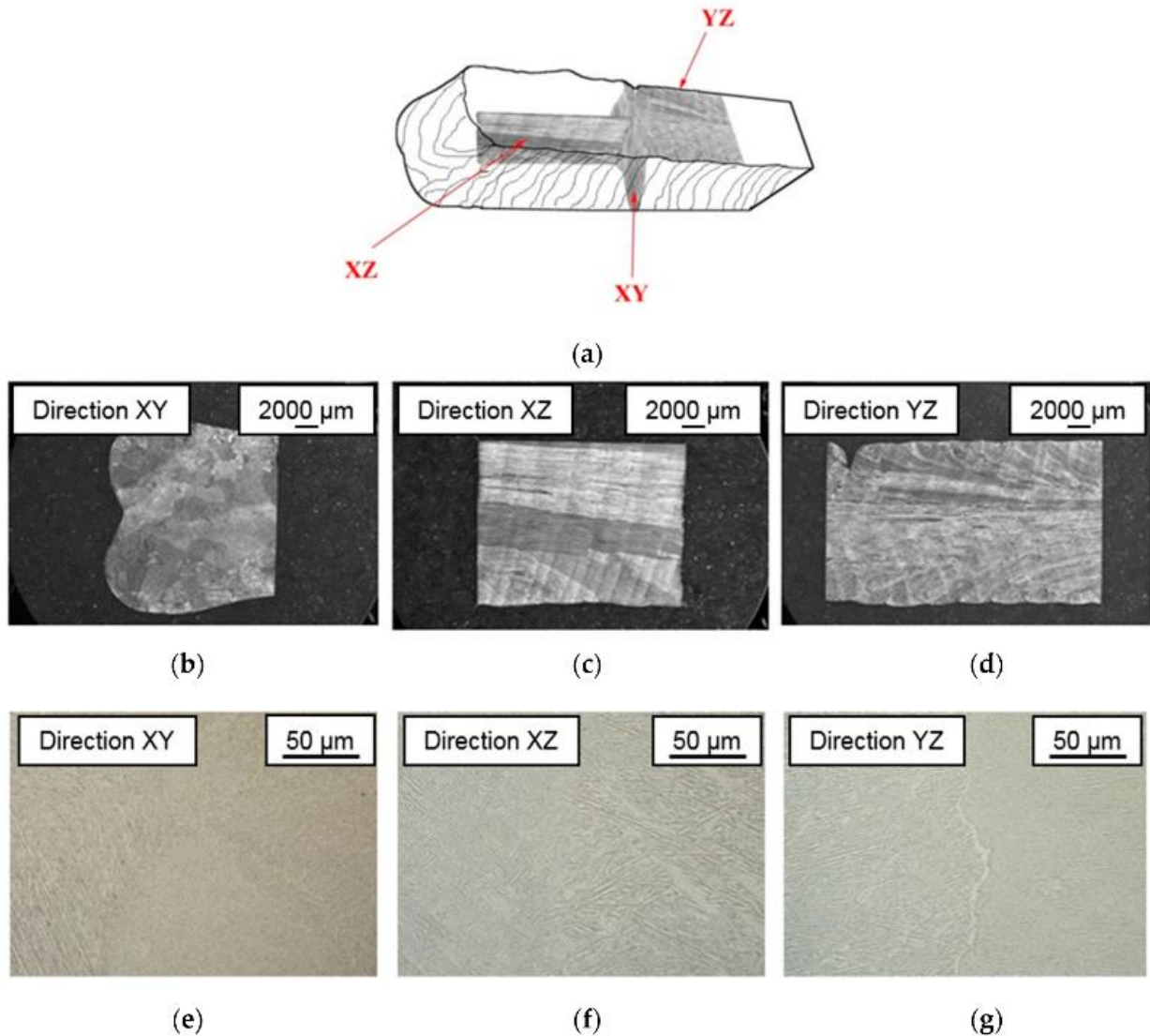

Hybrid additive-subtractive manufacturing processes combine the advantages of metal additive manufacturing with the high accuracy of machining processes [58]. Among these technologies, combining WAAM or PAW with milling presents the most promising option. Compared to additive laser technologies, this approach requires less investment in terms of both equipment and operation. Furthermore, WAAM operations can be implemented on existing milling machines through simple modernization to enable arc welding capabilities. The primary challenges associated with hybrid additive-subtractive processes are twofold. From a surfacing perspective, excessive heat input can induce significant deformations, residual stresses, and even catastrophic structural failure of the workpiece. Conversely, from a milling standpoint,

difficulties arise due to the poor machinability of the surfaced material, compounded by the inherent complexities of machining thin-walled components.

A single platform designed for hybrid additive and subtractive processes (WHASP) typically accommodates two or more workstations [59]. They integrate additive surfacing (DED, PAW) with subtractive CNC machining into a highly mobile, multi-axis machine tool (Fig. 7a). Enhanced numerical control (NC) and computer-aided design (CAD), manufacturing (CAM), and inspection (CAI) systems facilitate process control. A hybrid rolling-welding process is employed to mitigate residual stresses (Fig. 7b) [48].

FIGURE 7
SCHEMES OF DIFFERENT HYBRID 3D PRINTING PROCESSES: (A) ADDITIVE-SUBTRACTIVE POWDER-BASED PAW PROCESS WITH 3-5 AXIS CNC MILLING [59]; (B) ROLLING-WELDING PROCESS [48]
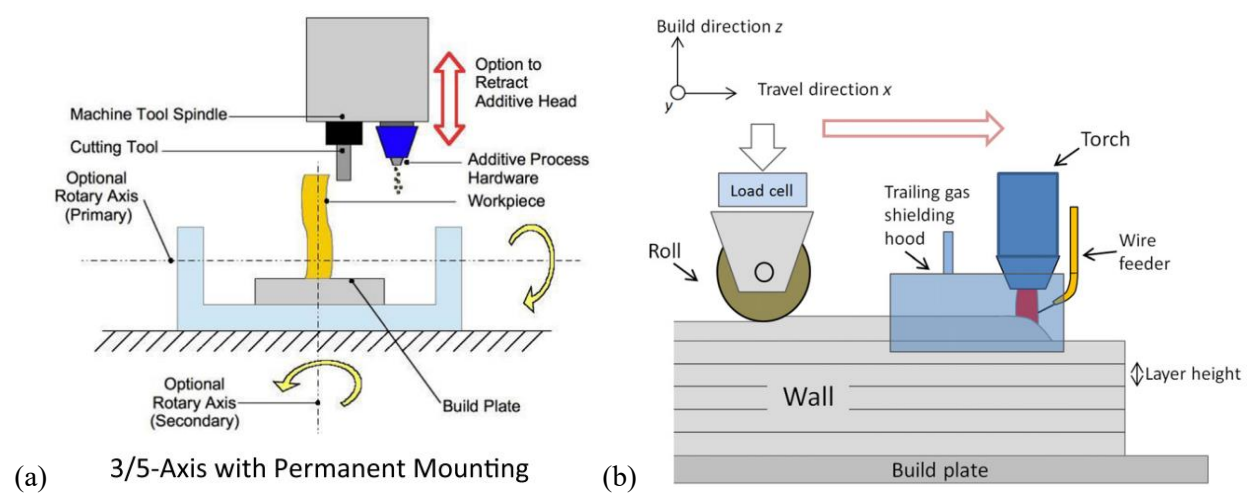
In addition to machining, hybrid and combined 3D printing processes for metal products include those that combine plasma heating with additional factors such as deformation processing (e.g., forging, rolling), pulsed energy sources, and supplemental heat treatments. For example, heat treatment during the aging process can be applied to enhance the strength of printed aluminum alloy products [60].

EXAMPLES OF PRACTICAL APTAS TECHNOLOGY APPLICATIONS IN MANUFACTURING (INCLUDING AEROSPACE STRUCTURES) AND NEW PERSPECTIVES

In recent years, technologies and equipment have been developed that enable the 3D printing of modular gliders, unmanned aerial vehicles, solid-propellant rockets, etc. [61]. Such approaches are used for the preparation of various spacecraft components, such as satellites and rockets, using 3D printing technologies on Earth. For example, study [62] describes a method of 3D printing with a consumable electrode arc to manufacture rocket engine structures from 436 stainless steel. 3D printing technologies have also been developed for use in space, including 3D printing on orbiting platforms, space stations, and spacecraft for deep space exploration [63]. Ukrainian manufacturers of liquid-propellant rocket engines are also engaged in this relevant research and development. They have developed an industrial 3D printing technology for manufacturing cooling channels in such engine nozzles [64]. 3D printing also has other applications in the manufacture of various aerospace products [65]. Let's examine these in greater detail.

One example of the successful application of APTAS technologies is the aerospace company Norsk Titanium (Plattsburgh, Norway), which has been producing aircraft parts using high-tech industrial 3D printing machines since 2017 [66]. The parts printed by Norsk using the plasma-arc method with titanium

alloy filler wires have received federal approval for use in commercial Boeing aircraft (USA). The technologies employed are not only 75% more productive than traditional forging but also reduce titanium product manufacturing costs by 50-75% while requiring fewer resources. Currently, several other companies, including the British companies Renishaw and Stratasys, are joining Norsk in the 3D printing of aerospace products.

Equipment for implementing 3D printing processes can be developed by product manufacturers directly or by companies specializing in welding technologies. Indeed, Norsk has developed 3D printing machines, such as the MERKE IV RPD, specifically for the application of the Rapid Plasma Deposition (RPD) process. Camarc Additive's (USA), a specialized company, has developed APTAS processes for steels, niobium, titanium, and aluminum alloys. For these processes, they created the PAAWS (Plasma Arc Additive Wire System), which offers four axes of movement (X, Y, Z, and rotation) along with a liquid-cooled printing table. Printing within a $1000 \times 10000 \times 600$ mm work envelope can be conducted in a sealed chamber with a controlled inert atmosphere and real-time process monitoring. SBI (Austria) is another prominent manufacturer of 3D printing equipment. Their systems are engineered for fabricating components from titanium and aluminum alloys, austenitic and nickel-chromium steels, copper, bronze, and other metals using plasma arc additive manufacturing with wire feed.

Another example of the application of APTAS technologies is the aerospace company Relativity Space [67]. This company is currently conducting intensive work on 3D printing medium-heavy reusable Terran R rockets (Fig. 8). Alongside APTAS, they utilize traditional arc technology, which, while inferior in several aspects, is characterized by relatively low productivity [68].

FIGURE 8
3D PRINTING OF TERRAN R ROCKET BODY ELEMENTS: A) ARC PRINTING OF THE COVER; B) APTAS OF THE SHELL FRAGMENT

(A)

(B)
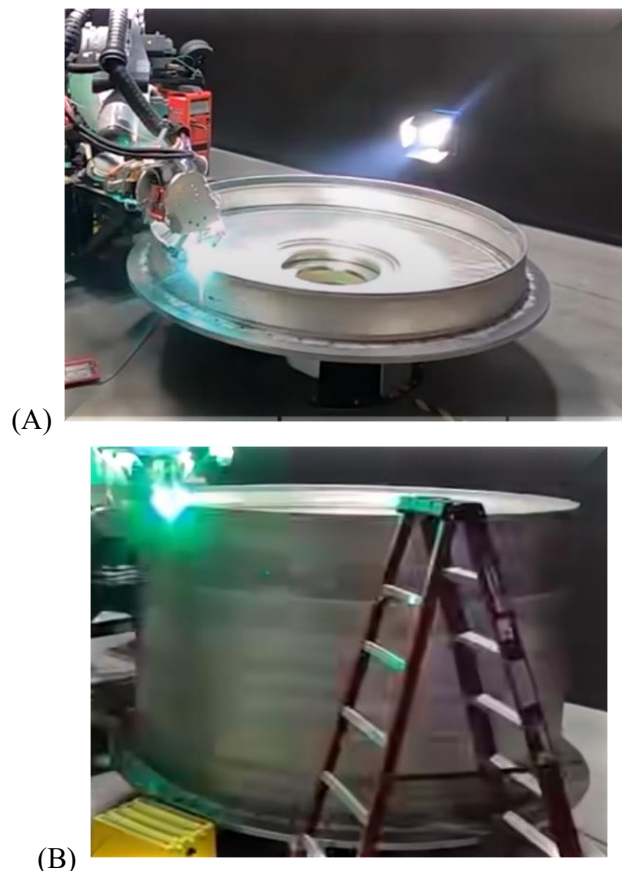
Research conducted at the E.O. Paton Electric Welding Institute of the National Academy of Sciences of Ukraine (EWI) [69] confirmed the possibility of synthesizing new high-strength alloys and smoothly changing the printed material's chemical composition in 3D printing. This can be achieved by using two or more dissimilar wires in the APTAS process, or by using wires and powder materials (Fig. 9, a).

Yes, studies conducted at the E.O. Paton Electric Welding Institute have shown that Hybrid 3D printing processes based on APTAS technology have enabled the fabrication of three-dimensional components composed of functionally graded metal matrix composites. These components exhibit spatially varying chemical compositions and reinforcement phase concentrations. An example application of these studies is the fabrication of three-dimensional products from a functionally graded "Ti-6Al-4V + WC" material. In these products, the tungsten carbide content varies from 0 to 50 wt.%, resulting in a Rockwell hardness ranging from 32 to 67 and above (Fig. 9b, c).

FIGURE 9
APTAS PROCESS (A) UTILIZING TI-6AL-4V WIRE AND WC POWDER, MICROSTRUCTURES OF CLADDING LAYERS PRODUCED WITH TI-6AL-4V WIRE AND WC POWDER (B), AND CLADDING WITH GRADIENT HARDNESS (C). 50 μM
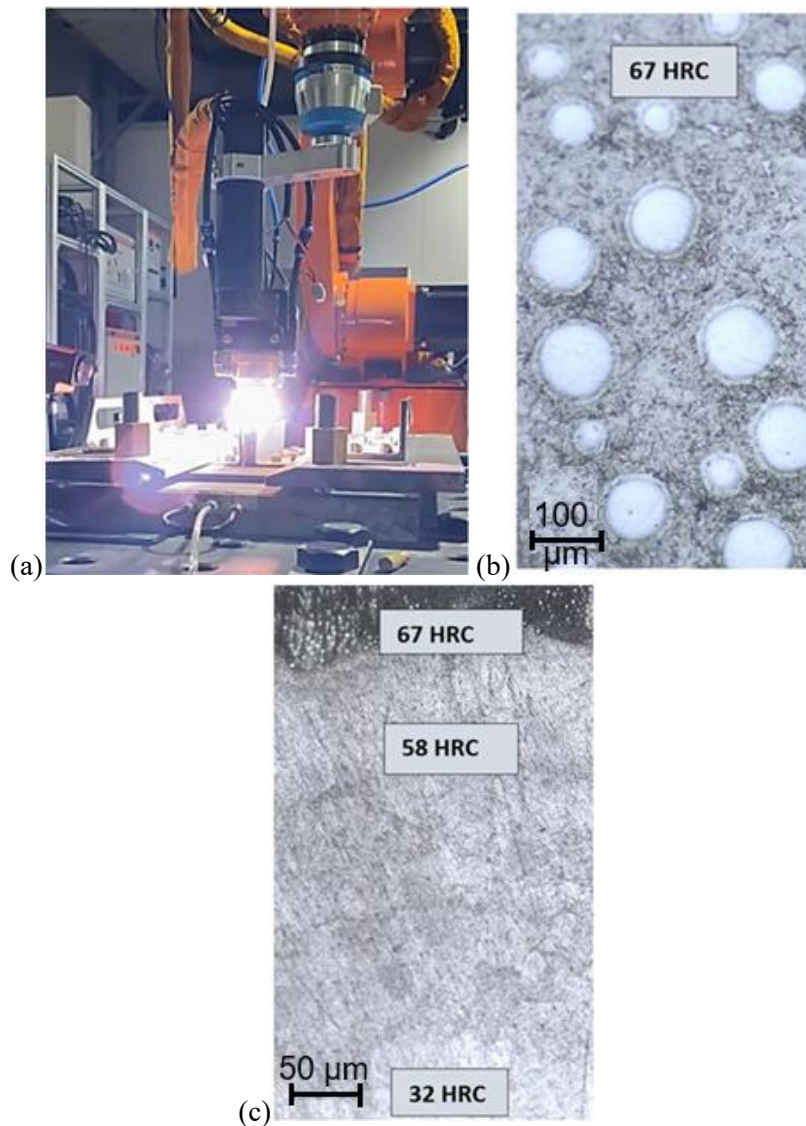
Developed at the E.O. Paton Electric Welding Institute, the robotic system for 3D printing of large-scale parts utilizes hybrid APTAS with wire and powder. This system enables the printing of elongated parts and bodies of revolution with dimensions up to 3000 mm in length, 600 mm in diameter, 600 mm in width, and 1000 mm in height (Fig. 10). The maximum printable workpiece weight is 1000 kg. This installation is implemented at the Institute of Welding in Hangzhou, PRC.

FIGURE 10
AN INSTALLATION FOR 3D PRINTING OF LARGE-SCALE PARTS USING HYBRID PLASMA TRANSFERRED ARC SURFACING WITH WIRE AND POWDER, DEVELOPED AT THE E.O. PATON ELECTRIC WELDING INSTITUTE

The plasma transferred arc surfacing equipment, integrated into the comprehensive 3D printing system for large-scale products, enables operation with both direct current of straight polarity and asymmetric alternating current with a frequency of up to 200 Hz. This ensures modulation of the welding current at a frequency of up to 20 Hz (for alternating current) and up to 2000 Hz (for direct current). A specialized equipment control system within the complex enables synchronized activation of the filler wire feed mechanism and the powder feed mechanism. The equipment complex facilitates APTAS implementation using nine degrees of freedom for tool and part movement.

In addition to the implemented 3D printing equipment, the E.O. Paton Electric Welding Institute is planning several new developments. Specifically, the authors have created a project design for a section with robotic complexes for 3D printing long (several meters or more) cylindrical shells (100–200 mm to several meters in diameter). These shells will feature elements and internal stiffeners of complex shapes (Fig. 11). This section also includes a robotic line for 3D printing long (4–12 meters) structures with complex profiles. These structures, made from aluminum and titanium alloys for aerospace applications, include stringers, spars, center wing beams, box-shaped structures with internal stiffeners, etc. The APTAS and CMT processes have been developed for 3D printing on this complex.

FIGURE 11
GENERAL VIEW OF THE ROBOTIC 3D PRINTING SITE FOR LONG AND LARGE METAL STRUCTURES

One of the main processes for printing 3D products from aluminum, magnesium, and other light alloys on the designed complex is additive plasma (microplasma) surfacing. This process utilizes an asymmetric alternating current ranging from 15 to 320 A, allowing for independent selection of the waveform during both direct and reverse polarity half-cycles. It also incorporates pulsed supply of the plasma-forming gas (argon) and pulsed filler wire feeding. Simultaneously, it is possible to utilize between one and four filler wires. Additionally, the application of filler powder materials is possible, both independently and in conjunction with wires. This APTAS implementation facilitates cathode cleaning, ensuring superior quality in the formation of deposited layers. This results in a finer microstructure and enhanced mechanical properties of both the deposited metal and the final products. The E.O. Paton Electric Welding Institute is also developing APTAS technologies for alloyed and high-strength steels, titanium, nickel, and copper alloys, as well as refractory metals. This process utilizes a direct current plasma arc with superimposed frequency modulation and preheating of the filler wire using an alternating asymmetric current.

Further prospects for the practical application of additive 3D printing technologies include developing plasma arc technologies for fabricating products with gradient functional properties and products composed of dissimilar materials. Specifically, APTAS technologies will enable this by combining wire and powder-based printing. Both the 3D printing of large structures and small, geometrically complex parts, including transition parts made from dissimilar materials, are promising. Realizing these prospects necessitates the development and implementation of intelligent software systems for automating 3D printing processes. These systems, through continuous, automated monitoring, will minimize characteristic defects in deposited layers and the residual stress-strain state of finished products.

## NEW POSSIBILITIES FOR APPLYING APTAS TECHNOLOGIES IN ADDITIVE MANUFACTURING

In the modern world, a new ideology of additive manufacturing is increasingly being proposed: the use of functionally graded materials (FGM). This has become one of the most relevant areas of research [70]. For the additive manufacturing of functionally graded materials, APTAS is used, particularly with two wires and a feedback mechanism [71]. This technology was used for 3D printing of Inconel 625 Ni–Cu products with a functional gradient.

Damage-tolerant, high-toughness ceramics are highly desirable for a variety of practical applications due to their unique combination of chemical and mechanical properties. However, current machining technologies do not allow for the creation of parts with complex or custom geometries from these materials.

However, additive manufacturing enables the fabrication of geometrically complex ceramic composite parts with exceptional damage resistance. Ceramic composite dental prostheses fabricated using the APTAS method avoid catastrophic failure, demonstrate a significant (approximately 116-fold) increase in strength compared to pure ceramics, and possess a customized geometry unattainable through conventional methods [72].

Research into natural cellular metamaterials has spurred global innovations utilizing homogeneous and heterogeneous materials to create structures with enhanced functionality. Additive manufacturing, including APTAS, enables the creation of complex geometries using multiple materials. This process provides additional functionality, environmental adaptability, and improved mechanical properties. Several studies have recently been conducted on multi-material additive manufacturing (MMAM) technologies, encompassing multi-materials, methodologies, design, and optimization [73]. MMAM technologies are particularly applicable to the fabrication of products from materials such as metal-metal (including those with specialized cellular macrostructures and microstructures), metal-ceramic (including those with alternating layers), metal-polymer, and multi-materials with functional gradations (Fig. 12).

FIGURE 12
EXAMPLES OF 3D-PRINTED METAL SAMPLES WITH A FUNCTIONAL GRADIENT [73]
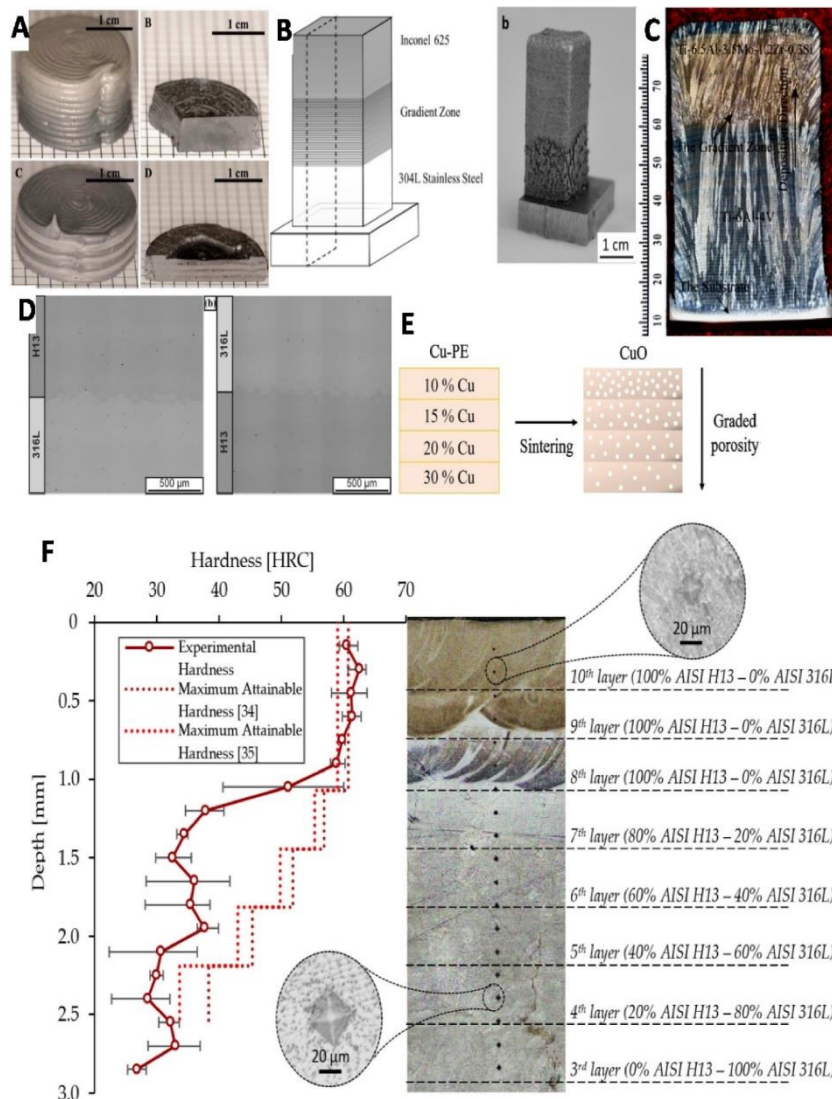
To obtain new alloys, control the chemical composition of bulk materials during 3D printing, and enhance printing productivity, multiple filler wires are fed into the system, sometimes in combination with granular materials (shot or powders).

To further refine the grain structure and reduce porosity in metal layers deposited via the APTAS method, ultrasonic surface treatment is employed [74]. For this purpose, an ultrasonic processing source configuration with a frequency of 40 kHz and a power of 60 W was selected. This source was found to mitigate hot cracking during combined ultrasonic additive manufacturing. This is achieved through supercooling during solidification, facilitated by a reduction in the temperature gradient within the melt pool. The grains in the treated layers exhibited an orientation perpendicular to the direction of vibration. More effective approaches to achieving similar structural modifications could include electrodynamic treatment of the deposited metal or modulation of the energy source [75, 76].

CONCLUSIONS

1. The additive manufacturing process for aerospace components utilizing compressed arc energy (APTAS) can employ both powder and wire feeding methods. The higher energy concentration within the APTAS heating spot, compared to the TIG process, facilitates the fabrication of narrower walls (from 3 mm) and a greater volume of deposited metal. Additionally, spatter defects are minimized in comparison to MIG/MAG processes. In terms of productivity, APTAS surfacing rivals MIG/MAG processes. In terms of accuracy and surface roughness, it approximates beam processes (SLM, EBSM) when utilizing the microplasma variant of APTAS. The economic efficiency of APTAS, compared to traditional aircraft engine component manufacturing methods, is 20-30%.
2. During the APTAS process for large-scale products composed of steels and iron- and nickel-based alloys, the layer structure develops with some height-wise heterogeneity due to heat dissipation into the substrate upon which the product is built. Overall, the structure is fine-grained and uniform, exhibiting minimal layer mixing. Dimensional deviations during the fabrication of large-scale components can be stabilized within ±0.5 mm, and porosity within 1-2%. The mechanical strength approximates 90-95% of cast metal.
3. For the additive cladding of large-scale products made from aluminum alloys, it is advisable to use APTAS with two or more wires. By adjusting the feed rate of each wire, the ratio of the main alloying elements (e.g., Mg and Cu) can be modified to obtain an alloy with a predictable chemical composition.
4. The WAAM process, utilizing a non-consumable electrode arc as the melting source for the filler wire, is employed for the additive cladding of large-scale products made from titanium alloys. The APTAS process offers the most promising option, as its compressed arc provides enhanced thermal locality and increased productivity compared to the TIG process.
5. Hybrid additive-subtractive manufacturing processes leverage the benefits of additive metal cladding alongside the high precision offered by concurrent machining. Furthermore, hybrid and combined 3D printing processes for metal products encompass those that integrate plasma heating with concurrent forming operations (e.g., forging, rolling), pulsed energy source modulation, supplementary heat treatments, and other techniques.
6. New opportunities for APTAS application in the aerospace industry include the development of technologies for fabricating products with functionally graded materials, dissimilar materials, and in-situ modification of the deposited metal using ultrasonic or electrodynamic treatment. APTAS technologies, through the combination of wire and powder feedstock, will not only increase productivity and economic efficiency but also enable the creation of novel alloys and the control of chemical composition within the bulk material during the 3D printing of aerospace structures and components.

AUTHOR CONTRIBUTIONS

ACKNOWLEDGMENTS

REFERENCES

[1.] Peleshenko, S., Korzhyk, V., Voitenko, O., Khaskin, V., & Tkachuk, V. (2017). Analysis of the current state of additive welding technologies for manufacturing volume metallic products (review). *Eastern European Journal of Enterprise Technologies*, *3/1*(87), 42–52. https://doi.org/10.15587/1729-4061.2017.99666

[2.] Borisov Yu.S., Kunitskii Yu.A., Korzhik V.N., & Yaprakova M.G. (1986). Structure and some physical properties of plasma-sprayed coatings of thenickel boride NiB. *Soviet Powder Metallurgy and Metal Ceramics*, *25*(12), 966–969.

[3.] Mao D., Xie Y., Meng X., Ma X., Zhang Z., Sun X., Wan L., . . . Huang Y. (2024). Strength-ductility materials by engineering a coherent interface at in coherent precipitates. *Materials Horizons*, *11*(14), 3408–3419. https://doi.org/10.1039/D4MH00139G

[4.] Antonysamy, A.A. (2012). *Microstructure, Texture and Mechanical Property Evolution during Additive Manufacturing of Ti6Al4V Alloy for Aerospace Applications: Microstructure*. (Doctoral dissertation). University of Manchester, Faculty of Engineering and Physical Sciences.

[5.] Mattox, J.M. (2013). Additive Manufacturing and its Implications for Military Ethics. *Journal of Military Ethics*, *12*(3), 225–234. https://doi.org/10.1080/15027570.2013.847534

[6.] Fialko, N., Dinzhos, R., Sherenkovskii, J., Meranova, N., Aloshko, S., Izvorska, D., . . . Nedbaievska, L. (2021). Establishment of regularities of influence on the specific heat capacity and thermal diffusivity of polymer nanocomposites of a complex of defining parameters. *Eastern-European Journal of Enterprise Technologies*, (114), 34–39. https://doi.org/10.15587/1729-4061.2021.245274

[7.] Korzhik V.N. (1992). Theoretical analysis of amorphization conditions for metallic alloys under gas-thermal spraying. III. Transformations in the amorphized alloy underbuilding-up of coatings. *Poroshkovaya Metallurgiya*, *11*, 47–52.

[8.] Fialko, N., Dinzhos, R., Sherenkovskii, J., Meranova, N., Prokopov, V., Babak, V., . . . Makhrovskyi, V. (2022). Influence on the thermophysical properties of nanocomposites of the duration of mixing of components in the polymer melt. *Eastern-European Journal of Enterprise Technologies*, *2*(5–116), 25–30. https://doi.org/10.15587/1729-4061.2022.255830

[9.] Alberti, E.A., Bueno, B.M.P., & D'Oliveira, A.S.C.M. (2016). Additive manufacturing using plasma transferred arc. *The International Journal of Advanced Manufacturing Technology*, *83*, 9–12. https://doi.org/10.1007/s00170-015-7697-7

[10.] Skorokhod, A.Z., Sviridova, I.S., & Korzhik, V.N. (1995). The effect of mechanical pretreatment of polyethylene terephthalate powderon the structural and mechanical properties of coatings made from it. *Mechanics of Composite Materials*, *30*(4), 328–334. https://doi.org/10.1007/BF00634755

[11.] Prokopov, V.G., Fialko, N.M., Sherenkovskaya, G.P., Yurchuk, V.L., S.Borisov, Yu., Murashov, A.P., & Korzhik, V.N. (1993). Effect of coating porosity on the process of heat transfer with gas-thermal deposition. *Powder Metallurgy and Metal Ceramics*, *32*, 118–121. https://doi.org/10.1007/BF00560034

[12.] Fialko, N.M., Prokopov, V.G., Meranova, N.O. et al. (1994). Temperature conditions of particle-substrate systems in a gas-thermaldeposition process. *Fizika i Khimiya Obrabotki Materialov*, *2*, 59–67.

[13.] Balushok, K., & Chigileychik, S. (2024). The scope of application of additive technologies by the method of plasma surfacing in the manufacture of aircraft engines. *Aerospace Technic and Technology*, (6), 47–51. https://doi.org/10.32620/aktt.2024.6.04

[14.] Fialko, N.M., Prokopov, V.G., Meranov, N.O., Borisov, Yu.S., Korzhik, V.N., & Sherenkovskaya, G.P. (1994). Temperature conditions of particle-substrate systems in a gas-thermal deposition process. *Fizika i Khimiya Obrabotki Materialov*, *2*, 59–67.

[15.] Fialko, N., Prokopov, V., Meranov N., et al. (1993). Thermal physics of gas thermal coatings formation processes. State of investigations. *Fizika i Khimiya Obrabotki Materialov*, *4*, 83–93.

[16.] Laue, R., Colditz, P., Möckel, M., & Awiszus, B. (2022). Study on the Milling of Additive Manufactured Components. *Metals*, *12*, 1167. https://doi.org/10.3390/met12071167

[17.] Gu, Y., Zhang, W., Xu, Y., et al. (2022). Stress-assisted corrosion behaviour of Hastelloy N in FLiNaK molten salt environment. *npj Mater Degrad*, *6*(90). https://doi.org/10.1038/s41529-022-00300-x

[18.] Prokopov, V.G., Fialko, N.M., Sherenkovskaya, G.P., Yurchuk, V.L., Borisov, Yu.S., Murashov, A.P., & Korzhik, V.N. (1993). Effect of the coating porosity on the processes of heat transfer under, gas-thermal atomization. *Poroshkovaya Metallurgiya*, *2*, 22–26.

[19.] Colegrove P., & Williams S. (2013). *High deposition rate high quality metal additive manufacture using wire + arc technology*. Cranfield University, 2013. Retrieved from https://www.xyzist.com/wp-content/uploads/2013/12/Paul-Colegrove-Cranfield-Additive-manufacturing.pdf

[20.] Özel, T., Shokri, H., & Loizeau, R. (2023). A Review on Wire-Fed Directed Energy Deposition Based Metal Additive Manufacturing. *Manuf. Mater. Process.*, *7*, 45. https://doi.org/10.3390/jmmp7010045

[21.] Fialko, N., Dinzhos, R., Sherenkovskii, J., Meranova, N., Aloshko, S., Izvorska, D., . . . Nedbaievska, L. (2021). Establishment of regularities of influence on the specific heat capacity and thermal diffusivity of polymer nanocomposites of a complex of defining parameters. *Eastern-European Journal of Enterprise Technologies*, *6*(12(114)), 6–12. http://dx.doi.org/10.15587/1729-4061.2021.245274

[22.] Pershin V., Lufitha M., Chandra S., et al. (2003). Effect of substrate temperature on adhesion strength of plasma-sprayed nickel coatings. *Journal of Thermal Spray Technology*, *12*, 370–376. https://doi.org/10.1361/105996303770348249

[23.] Ge, J., Lin, J., Lei, Y., & Fu, H. (2017). Location-related Thermal History, Microstructure, and Mechanical Properties of Arc Additively Manufactured 2Cr13 Steel Using Cold Metal Transfer Welding. *Materials Science & Engineering A*, 12.076. https://doi.org/10.1016/j.msea.2017.12.076

[24.] Treutler, K. (2023). Plasma Powder Transferred Arc Additive Manufacturing of ((Fe,Ni)-Al) Intermetallic Alloy and Resulting Properties. *Research Square*, 24 p. Preprint CC BY 4.0. https://doi.org/10.21203/rs.3.rs-3042098/v1

[25.] Alaluss, K., & Mayr, P. (2019). Additive Manufacturing of Complex Components through 3D Plasma Metal Deposition – A Simulative Approach. *Metals*, *9*(5), 574. https://doi.org/10.3390/met9050574

[26.] Fialko, N., Dinzhos, R., Sherenkovskii, J., Meranova, N., Navrodska, R., Izvorska, D., . . . Koseva, N. (2021). Establishing Patterns In The Effect Of Temperature Regime When Manufacturing Nanocomposites On Their Heat-Conducting Properties. *Eastern-European Journal of Enterprise Technologies*, *4*(5(112)), 21–26. http://dx.doi.org/10.15587/1729-4061.2021.236915

[27.] Fialko, N., Prokopov, V., Meranova, N., et al. (1993). Thermal physics of gas thermal coatings formation processes. State of investigations. *Fizika i Khimiya Obrabotki Materialov*, *4*, 83–93.

[28.] Fialko, N., Prokopov, V., Meranova, N., et al. (1994). Temperature conditions of particle-substrate systems in a gas-thermal deposition process. *Fizika i Khimiya Obrabotki Materialov*, *2*, 59–67.

[29.] Alhuzaim A.F. (2014). *Investigation in the Use of Plasma Arc Welding and Alternative Feedstock Delivery Method in Additive Manufacture: Master of Science General Engineering.* Montana Tech of the University of Montana, 228 p.

[30.] Skorokhod A.Z., Sviridova I.S., & Korzhik V.N. (1994). Structural and mechanical properties of polyethylene terephthalatecoatings as affected by mechanical pretreatment of powder in the course of preparation. *Mekhanika Kompozitnykh Materialov*, *30*(4), 455–463.

[31.] Alaluss, K., & Mayr, P. (2019). Additive Manufacturing of Complex Components through 3D Plasma Metal Deposition – A Simulative Approach. *Metals*, *9*(5), 574. https://doi.org/10.3390/met9050574

[32.] Gnatenko, M., Chigileichyk, S., & Sakhno, S. (2021). Manufacture of aviation parts from heat-related nickel alloys by multilayer plasma surfacing. *Aerospace Technic and Technology*, 5, 48–52. https://doi.org/10.32620/aktt.2021.5.06

[33.] Balushok, K., Chigileychik, S., Petryk, I., Sakhno, S., & Kulykovskyi, R. (2024). Developing Technology of Directed Energy Deposition of Workpieces of Aircraft Engines from Heat-Resistant Nickel Alloys by Means of Using Layer-by-Layer Microplasma Surfacing Method. *Mechanics and Advanced Technologies*, *8*(2), 121–129. https://doi.org/10.20535.2521-1943.2024.8.2(101).296932

[34.] Chigileychik, S., Torba, Y., Kulykovskyi, R., Shyrokobokova, N., & Chechet O. (2024). Infuence of active gas content in powder on mechanical properties of workpiece blanks produced by plasma additive technologies. *New Materials and Technologies in Metallurgy and Mechanical Engineering*, (4), 52–56. https://doi.org/10/15588/1607-6885-2024-4-5

[35.] Yushchenko, K.A., Yarovytsyn, O.V., Khrushchov, G.D., Petrik, I.A., & Chygileichyk, S.L. (2022). Optimization of refurbishment of HPT blades of the D-18T aircraft gas turbine engine by micro-plasma powder welding. *Space Science and Technology*, *28*(3), 3–16. https://doi.org/10.15407/knit2022.03.003

[36.] Chigileychik, S., Petrik, I.A., Ovchinnikov, A., & Kyrylakha S. (2022). Experience in implementing additive technologies during repair of GTE parts from alloy EP 648 VI (KHN50VMTYUB-VI) under conditions of serial production. *Aerospace Technic and Technology*, (1), 57–63. https://doi.org/10.32620/aktt.2022.1.07

[37.] Gnatenko, M. (2024). Elimination of casting defects of parts by microplasma surfacing methods. *Mining Bulletin*, *22*(1), 126–130. https://doi.org/10.31721/2306-5435-2024-1-112-126-130

[38.] Geng, H., Li, J., Xiong, J., Lin, X., & Zhang, F. (2017). Geometric Limitation and Tensile Properties of Wire and Arc Additive Manufacturing 5A06 Aluminum Alloy Parts. *Journal of Materials Engineering and Performance*, *26*, 621–629. https://doi.org/10.1007/s11665-016-2480-y

[39.] Bai, J.Y., Yang, C.L., Lin, S.B., Dong, B.L., & Fan, C.L. (2016). Mechanical properties of 2219-Al components produced by additive manufacturing with TIG. *Int. J. Adv. Manuf. Technol.*, *86*, 479–485. https://doi.org/10.1007/s00170-015-8168-x

[40.] Geng, H., Li, J., Xiong, J., Lin, X., & Zhang, F. (2017). Optimization of wire feed for GTAW based additive manufacturing. *Journal of Materials Processing Technology*, *243*, 40–47. http://dx.doi.org/10.1016/j.jmatprotec.2016.11.027

[41.] Qi, Z., Cong, B., Qi, B., Sun, H., Zhao, G., & Ding, J. (2018). Microstructure and mechanical properties of double-wire + arc additively manufactured Al-Cu-Mg alloys. *Journal of Materials Processing Technology*, *255*, 347–353. https://doi.org/10.1016/j.jmatprotec.2017.12.019

[42.] Reisgen, U., Sharma, R., Oster, L., & Zanders E. (2018, September 16–17). Plasma-Mehrdraht-Schweißen zum Herstellen gradierter Strukturen. In *Proceedings of the DVS CONGRESS*, pp.109–114. (In German). Friedrichshafen, Germany.

[43.] Martina, F., Mehnen, J., Williams, S.W., Colegrove, P., & Wang, F. (2012). Investigation of the benefits of plasma deposition for the additive layer manufacture of Ti-6Al-4V. *Journal of Materials Processing Technology*, *212*(6), 1377–1386.

[44.] Williams, S.W., Martina, F., Addison, A.C., Ding, J., Pardal, G., & Colegrove, P. (2016). Wire + Arc Additive Manufacturing. *Materials Science and Technology*, *32*(7), 641–647. https://doi.org/10.1179/1743284715Y. 0000000073

[45.] Colegrove, P.A., Martina, F., Roy, M.J., Szost, B.A., Terzi, S., Williams, S.W., . . . Jarvis, D. (2014). High pressure interpass rolling of wire + arc additively manufactured titanium components. *Advanced Materials Research*, *996*, 694–700. https://doi.org/10.4028/www.scientific.net/AMR.996.694

[46.] Martina, F., Roy, M.J., Szost, B.A., Terzi, S., Colegrove, P.A., Williams, S.W., . . . Hofmann, M. (2016). Residual stress of as-deposited and rolled wire + arc additive manufacturing Ti–6Al–4V components. *Materials Science and Technology*, *32*(14), 1439–1448. http://dx.doi.org/10.1080/02670836.2016.1142704

[47.] Moztarzadeh, H., Hughes, D.J., Seth, S., Keating, E., Kiraci, E., Gibbons, G.J., & Dashwood, R.J. (2015). Evolution of residual stresses in linear deposition wire-based cladding of Ti-6Al-4V. In *8th International Conference on Mechanical Stress Evaluation by Neutron & Synchrotron Radiation MACASENS 2015*, Grenoble, France, 30 Sep.–2 Oct. 2015. 7 p. Published in: Materials Science Forum (In Press). Retrieved from http://wrap.warwick.ac.uk/78892

[48.] Donoghue, J., Antonysamy, A.A., Martina, F., Colegrove, P.A., Williams, S.W., & Prangnell, P.B. (2016). The effectiveness of combining rolling deformation withWire–Arc Additive Manufacture on β-grain refinement and texture modification in Ti–6Al–4V. *Materials Characterization*, *114*, 103–114. http://dx.doi.org/10.1016/j.matchar.2016.02.001

[49.] Wu, B., Ding, D., Pan, Z., Cuiuri, D., Li, H., Han, J., & Fei, Z. (2017). Effects of heat accumulation on the arc characteristics and metal transfer behavior in Wire Arc Additive Manufacturing of Ti6Al4V. *Journal of Materials Processing Technology*, *250*, 304–312. http://dx.doi.org/10.1016/j.jmatprotec.2017.07.037

[50.] Wua, B., Pana, Z., Dingb, D., Cuiuria, D., Lia, H., & Feia, Z. (2018). The effects of forced interpass cooling on the material properties of wire arc additively manufactured Ti6Al4V alloy. *Journal of Materials Processing Technology*, *258*, 97–105. https://doi.org/10.1016/j.jmatprotec.2018.03.024

[51.] Hoefer, K., & Mayr, P. (2018). Additive Manufacturing of Titanium Parts Using 3D Plasma Metal Deposition. *Materials Science Forum*, *941*, 213–2141. http://dx.doi.org/10.4028/www.scientific.net/MSF.941.2137

[52.] R´ıos, S., Colegrove, P.A., & Williams, S.W. (2019). Metal Transfer Modes in plasma Wire + Arc Additive Manufacture. *Journal of Materials Processing Tech*, *264*, 45–54. https://doi.org/10.1016/j.jmatprotec.2018.08.043

[53.] Lin, Z., Song, K., & Yu, X. (2021). A review on wire and arc additive manufacturing of titanium alloy. *Journal of Manufacturing Processes*, *70*, 24–45. https://doi.org/10.1016/j.jmapro.2021.08.018

[54.] Xionga, X., Zhang, H., Wang, G., & Wang G. (2010). Hybrid plasma deposition and milling for an aeroengine double helix integral impeller made of superalloy. *Robotics and Computer-Integrated Manufacturing*, *26*, 291–295. https://doi.org/10.1016/j.rcim.2009.10.002

[55.] Zhang, H., Xu, J., & Wang, G. (2003). Fundamental study on plasma deposition manufacturing. *Surface and Coatings Technology*, *171*, 112–118. https://doi.org/10.1016/S0257-8972(03)00250-0

[56.] Sun, J., Yu, H., Zeng, D., & Shen, P. (2022). Wire–powder–arc additive manufacturing: A viable strategy to fabricate carbide ceramic/aluminum alloy multi-material structures. *Additive Manufacturing*, *51*, 102637. https://doi.org/10.1016/j.addma.2022.102637

[57.] Veiga F., Gil Del Val A., Suárez A., Alonso U. (2020). Analysis of the Machining Process of Titanium Ti6Al-4V Parts Manufactured by Wire Arc Additive Manufacturing (WAAM). *Materials*, *13*(3), 766. https://doi.org/10.3390/ma13030766

[58.] Montevecchi, F. (2017). Analysis and optimization of hybrid WAAM-milling process. Doctoral programme in industrial engineering. Università degli Studi di Firenze, Italy. 172 p.

[59.] Flynn, J.M., Shokrani, A., Newman, S.T., & Dhokia, V. (2016). Hybrid additive and subtractive machine tools – Research and industrial developments. *International Journal of Machine Tools and Manufacture*, *101*, 79–101.https://doi.org/10.1016/j.ijmachtools.2015.11.007

[60.] Yang, J., Ni, Y., Li, H., Fang, X., & Lu, B. (2023). Heat Treatment Optimization of 2219 Aluminum Alloy Fabricated by Wire-Arc Additive Manufacturing. *Coatings*, *13*, 610. https://doi.org/10.3390/coatings13030610

[61.] Hernandez, R.N., Singh, H., Messimer, S.L., & Patterson, A.E. (2017). Design and Performance of Modular 3-D Printed Solid-Propellant Rocket Airframes. *Aerospace*, *4*(2), 17. https://doi.org/10.3390/aerospace4020017

[62.] Thomas, D.J. (2022). Advanced active-gas 3D printing of 436 stainless steel for future rocket engine structure manufacture. *Journal of Manufacturing Processes*, *74*, 256–265. https://doi.org/10.1016/j.jmapro.2021.12.037

[63.] Li Y., Li X., & Shen D. (2024). 3D Printing of Artificial Satellites and Rockets. In *3D Printing in Space* (pp. 21–56). https://doi.org/10.1007/978-981-97-4094-9_3

[64.] Sirenko, M., & Karpovych E. (2023). Development prospects of 3d-printing of objects in aviation and aerosoace from polymer materials with composite reinforcement. *Journal of Rocket-Space Technology*, *30*(4), 9–14. https://doi.org/10.15421/452202

[65.] Vekilov S.S., Lipovskyi V., & Marchan R.A. (2021). Features of the adaptation of 3d printed regenerative cooling channels of the lpre throat inserts. *System Design and Analysis of Aerospace Technique Characteristics*, *29*(2), 62–72. https://doi.org/10.15421/472112

[66.] Norsk Titanium. (n.d.). *The future of manufacturing is rapid plasma deposition*. Retrieved from https://www.norsktitanium.com/

[67.] A potential rival to SpaceX and Blue Origin. Former Google CEO leads aerospace startup. (2025, March 11). *Relativity Space*. AIN. Retrieved from https://en.ain.ua/2025/03/11/ex-google-ceo-relativity-space/

[68.] Relativity: Meeting Market Demand. (n.d.). Terran R: Our Approach and Progress. Retrieved from https://www.relativityspace.com/terran-r

[69.] Korzhyk V.M., Grynyuk A.A., Khaskin V.Yu., Voitenko O.M., Burlachenko O.M., & Khuan O.O. (2023). Plasma-arc technologies of additive surfacing (3D printing) of spatial metal products: Application experience and new opportunities. *The Paton Welding Journal*, *11*, 3–20. https://doi.org/10.37434/tpwj2023.11.01

[70.] Ma Z., Liu W., Li W., Liu H., Song J., Liu Y., . . . Zhang Y. (2024). Additive manufacturing of functional gradient materials: A review of research progress and challenges. *Journal of Alloys and Compounds*, *971*, 172642. https://doi.org/10.1016/j.jallcom.2023.172642

[71.] Wang Y., Konovalov S., Chen X., Singh R. A., & Jayalakshmi S. (2022). Research on plasma arc additive manufacturing of Inconel 625 Ni–Cu functionally graded materials. *Materials Science and Engineering: A*, *853*, 143796. https://doi.org/10.1016/j.msea.2022.143796

[72.] Sun J., Yu S., Wade-Zhu J., Wang Y., Qu H., Zhao S., . . . Bai J. (2022). 3D printing of ceramic composite with biomimetic toughening design. *Additive Manufacturing*, *58*, 103027. https://doi.org/10.1016/j.addma.2022.103027

[73.] Nazir A., Gokcekaya O., Billah K. M. M., Ertugrul O., Jiang J., Sun J., . . . Hussain S. (2023). Multi-material additive manufacturing: A systematic review of design, properties, applications, challenges, and 3D printing of materials and cellular metamaterials. *Materials & Design*, *226*, 111661. https://doi.org/10.1016/j.matdes.2023.111661

[74.] Lowe P.S., Honey X., Crossley J., Karunaratne K., Kannangara C., & Jones S. (2022). Scaling-up ultrasonic vibration assisted additive manufacturing to build 316 L 3 m3 waste container flange. *Journal of Manufacturing Processes*, *83*, 97–104. https://doi.org/10.1016/j.jmapro.2022.08.053

[75.] Han J., Shi Y., Zhang G., Volodymyr K., & Le W.-Y. (2022). Minimizing defects and controlling the morphology of laser welded aluminum alloys using power modulation-based laser beam oscillation. *Journal of Manufacturing Processes*, *83*, 49–59. https://doi.org/10.1016/j.jmapro.2022.08.031

[76.] Gu Y., Xu Y., Shi Y., Feng C., & Volodymyr K. (2022). Corrosion resistance of 316 stainless steel in a simulated pressurized waterreactor improved by laser cladding with chromium. *Surface and Coatings Technology*, *441*, 128534. https://doi.org/10.1016/j.surfcoat.2022.128534